Charge carrier mobility and concentration as a function of composition in AgPO3–AgI glasses

Ana Candida Martins Rodrigues, Marcio Luis Ferreira Nascimento, Caio Barca Bragatto, and Jean-Louis Souquet

Related Articles

Additional information on J. Chem. Phys.

Charge carrier mobility and concentration as a function of composition in AgPO₃–AgI glasses

Ana Candida Martins Rodrigues,[1,a)] Marcio Luis Ferreira Nascimento,[2]
Caio Barca Bragatto,[1] and Jean-Louis Souquet[3]

[1]*Laboratório de Materiais Vítreos, Departamento de Engenharia de Materiais, Universidade Federal de São Carlos, 13565-905 São Carlos-SP, Brazil*
[2]*Instituto de Humanidades, Artes & Ciências, Universidade Federal da Bahia, Rua Barão de Jeremoabo s/n, PAF 3, Campus Universitário de Ondina, 40170-115 Salvador-BA, Brazil*
[3]*Laboratoire d'Electrochimie et de Physicochimie des Matériaux et des Interfaces, PHELMA, BP 75, 38402 Saint Martin D'Hères Cedex, France*

Conductivity data of the xAgI$(1 - x)$AgPO₃ system $(0 \leq x \leq 0.5)$ were collected in the liquid and glassy states. The difference in the dependence of ionic conductivity on temperature below and above their glass transition temperatures (T_g) is interpreted by a discontinuity in the charge carrier's mobility mechanisms. Charge carrier displacement occurs through an activated mechanism below T_g and through a Vogel-Fulcher-Tammann-Hesse mechanism above this temperature. Fitting conductivity data with the proposed model allows one to determine separately the enthalpies of charge carrier formation and migration. For the five investigated compositions, the enthalpy of charge carrier formation is found to decrease, with x, from 0.86 to 0.2 eV, while the migration enthalpy remains constant at ≈ 0.14 eV. Based on these values, the charge carrier mobility and concentration in the glassy state can then be calculated. Mobility values at room temperature $(\approx 10^{-4}$ cm² V⁻¹ s⁻¹$)$ do not vary significantly with the AgI content and are in good agreement with those previously measured by the Hall-effect technique. The observed increase in ionic conductivity with x would thus only be due to an increase in the effective charge carrier concentration. Considering AgI as a weak electrolyte, the change in the effective charge carrier concentration is justified and is correlated to the partial free energy of silver iodide forming a regular solution with AgPO₃. © *2011 American Institute of Physics*. [doi:10.1063/1.3666835]

I. INTRODUCTION

Silver conducting glasses are among the best known solid electrolytes and some compositions present a conductivity as high as 10^{-2} S cm⁻¹ at room temperature. Since their electrochemical window is narrow, these glasses remain of limited technological interest. However, they are prepared easily over a wide composition range and have been studied as model systems to understand the relationship between structural or thermodynamic characteristics and ionic transport. The results of these studies have later been applied to conceive new highly conducting lithium glasses for use as solid electrolytes in lithium batteries.[1,2]

The xAgI$(1 - x)$AgPO₃ glasses, in particular, with $0 \leq x \leq 0.5$ (x is the AgI molar fraction), have been investigated extensively by different electrical[3–10] or calorimetric[11–15] techniques, NMR,[16–20] Raman,[21,22] or IR[23] spectroscopy, and by Brillouin[24] and neutron[25–32] scattering. As confirmed by transport number measurements,[4] they are purely Ag⁺ conductive in the whole composition range. Their ionic transport is extremely sensitive to the silver iodide content, since, at room temperature, conductivity increases by more than four orders of magnitude, from 2×10^{-7} ($x = 0$) to 5×10^{-3}

S cm⁻¹ ($x = 0.5$), although the concentration of silver cations remains approximately constant in this composition range.

The ionic conductivity, σ, of all alkali and silver conducting glasses, is expressed as

$$\sigma = n_+ e \mu_+, \tag{1}$$

where n_+ is the effective charge carrier concentration, e is their positive charge, and μ_+ is their electrical mobility. However, the individual determination of charge carrier concentration and mobility remains an open question and a challenging subject in the field of ionic conduction in glass. Thus, the large isothermal variations in conductivity as a function of silver iodide content (x) may be attributed to major variations in either mobility or effective charge carrier concentration.

In the case of ionic transport in solids, only the Hall-effect technique allows for the unambiguous separation of the contributions of charge carrier mobility and concentration to conductivity. In ionic solids, this technique is difficult to apply due to the low Hall signal in solid electrolytes.[33,34] However, using an ac Hall technique on xAgI$(1 - x)$AgPO₃ glasses, Clément *et al.*[35] found an Ag⁺ mobility value, independent of x, of $(6 \pm 2) \times 10^{-4}$ cm² s⁻¹ V⁻¹ at 25 °C. Hence, it can be stated that the increase observed in conductivity with AgI content is more likely due to an increase in charge carrier concentration than in charge carrier mobility. The measured mobility also allows for the estimation of the (n_+/n) ratio, where

a)Author to whom correspondence should be addressed. Electronic mail: acmr@ufscar.br.

n_+ is the concentration of effective charge carriers and n is the total concentration of silver cations. Based on their mobility measurements, Clément *et al.*[35] found that, at room temperature, this ratio increased from 6×10^{-8} in pure $AgPO_3$ to 2×10^{-2} in the $x = 0.5$ composition.

Recently, we proposed another possibility to calculate both charge carrier mobility and concentration in ionic glasses, using conductivity data as a function of temperature below and above the glass transition temperature T_g.[36] This method, based on the discontinuity in the ionic transport mechanism between the glassy and supercooled liquid phases,[37] allows the concentration and mobility of charge carriers to be determined in a wide range of temperatures, below and above the glass transition temperature, whereas Hall-effect measurements are usually limited to room temperature.

In the present work, we applied the aforementioned method to previously published conductivity data on $AgPO_3-AgI$ melts and glasses, and, as a validity test, compared the mobility results with those obtained by Clément *et al.*[35] Variations in charge carrier concentration with AgI content are then interpreted based on the weak electrolyte model,[38,39] assuming a partial dissociation of silver iodide in the silver phosphate solvent glass.

II. A MODEL OF IONIC TRANSPORT IN THE SUPERCOOLED AND GLASSY STATES

For clarity, we summarize below the basic hypothesis of the model proposed in Ref. 36 and applied here to calculate the silver cation mobility and charge carrier concentration in the $x AgI(1 - x)AgPO_3$ system as a function of the halogenated salt, AgI, content.

From a microscopic standpoint, it has been proposed that cationic transport in glasses occurs by interstitial cationic pairs,[40–42] formed by two cations sharing the same negatively charged site. Note that, in the specific case of a phosphate, such a negatively charged site is constituted of an electronic charge delocalized between a phosphorus atom linked covalently to two oxygen atoms.

The formation of an interstitial cationic pair therefore results from the dissociation of a cation ionically bound to its site, allowing it to jump to a neighboring cationic site that is already occupied. Thus, the resulting site occupied by two alkali cations is positively charged.

The concentration n_+ of those sites, which represents the effective charge carrier concentration, depends on the total cation concentration, n, on the free energy $\Delta G_f = \Delta H_f - T \Delta S_f$ associated with the simultaneous formation of an interstitial pair and a cation vacancy, on the temperature, T, and on the Boltzmann constant, k_B. Since the contribution of the entropic term is negligible, as we will justify later, one can write

$$n_+ = n \exp\left(-\frac{\Delta H_f}{2k_B T}\right) \quad \text{or} \quad \frac{n_+}{n} = \exp\left(-\frac{\Delta H_f}{2k_B T}\right). \tag{2}$$

The excess cation may be transferred from one site to another, allowing for the migration of the positive charge in the macromolecular network of the glass former subjected to an electric field.

The corresponding mobility of the interstitial pair is, thus, a function of its characteristic attempt frequency ν, the jump distance λ, and the probability of a successful jump Ω:

$$\mu_+ = \frac{e\lambda^2 \nu}{6k_B T}\Omega. \tag{3}$$

In a thermally activated mechanism, $\Omega = \Omega_1$ is a function of the free energy required for migration, ΔG_m, which, if also restricted to the enthalpic term, can be expressed as

$$\Omega = \Omega_1 = \exp\left(-\frac{\Delta H_m}{k_B T}\right). \tag{4}$$

Finally, Eqs. (2)–(4) lead to the following expression for conductivity:

$$\sigma = en_+\mu_+ = n\frac{e^2\lambda^2 \nu}{6k_B T}\exp\left(-\frac{\Delta H_f/2 + \Delta H_m}{k_B T}\right), \tag{5}$$

which, considering the σT product to eliminate the temperature from the pre-exponential term, may be written as

$$\sigma T = A \exp(-E_A/k_B T) \tag{6}$$

with

$$A = n\frac{e^2\lambda^2 \nu}{6k_B}, \tag{6a}$$

$$E_A = \Delta H f/2 + \Delta H m. \tag{6b}$$

In an Arrhenius plot such as the one represented schematically in Figure 1, conductivity data below T_g define a straight line whose slope gives access to E_A, the activation energy for conduction, and the extrapolated value at $1/T = 0$ to the pre-exponential term A.
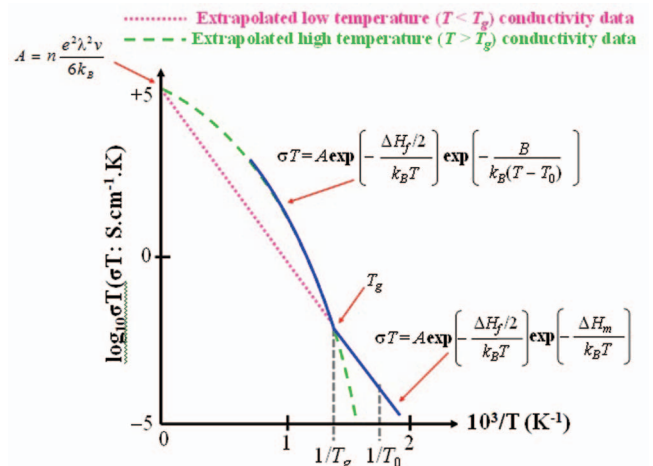

FIG. 1. Schematic representation of conductivity variation as a function of temperature. Below T_g, charge carrier formation and migration are both activated mechanisms. Above T_g, charge carrier formation remains activated but its migration, correlated with chain movements, follows a VFTH dependence on temperature.
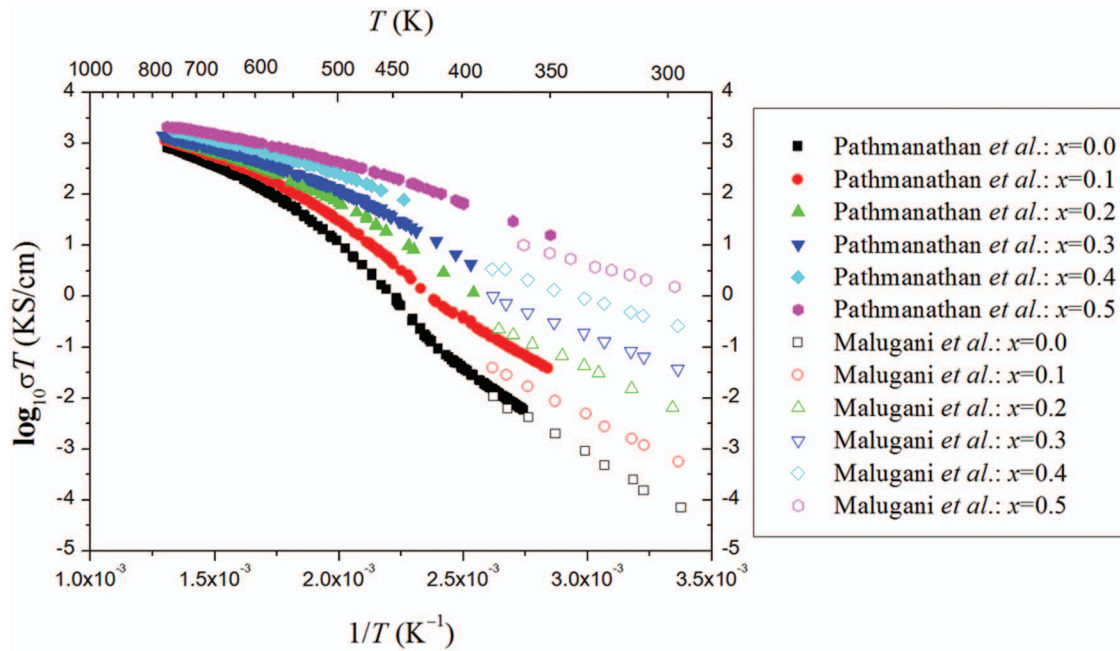
FIG. 2. σT product as a function of temperature in Arrhenius coordinates for five compositions of the xAgI$(1 - x)$AgPO$_3$ system. Open symbols represent experimental data from Malugani *et al.*,[4] and solid symbols represent data from Pathmanathan *et al.*[7]

Above the glass transition temperature, the migration mechanism is coupled to the chain movement. The jump probability of the excess cation may thus be described by a Vogel-Fulcher-Tamann-Hesse (VFTH) expression:

$$\Omega_2 = \exp\left[-\frac{B}{k_B(T - T_0)}\right], \tag{7}$$

where B and T_0 are constants in the temperature window under consideration. Their microscopic significance depends on the chosen description (free volume[43] or entropic model[44]) of the coupled movement of charge carrier and chain segments. Physically, T_0 is the temperature below which the chain segments no longer participate in charge carrier displacement. This is called the ideal glass transition temperature, which is linked to the measured glass transition temperature, T_g, by the semiempirical relation[37,45]

$$T_0 \approx \frac{3}{4}T_g. \tag{8}$$

Above T_g, migration by a VFTH mechanism prevails over the Arrhenius one (i.e., $\Omega_2 \gg \Omega_1$) and ionic conductivity can be written as

$$\sigma T = A \exp\left(-\frac{\Delta H_f/2}{k_B T}\right)\exp\left[-\frac{B}{k_B(T - T_0)}\right]. \tag{9}$$

This expression contains *a priori* four characteristic parameters of the glass forming melt, A, ΔH_f, B, and T_0. However, two of them can be reasonably estimated: A, from the extrapolation of the Arrhenius plot below T_g and T_0 by the semiempirical rule shown by Eq. (8). The fit of experimental data using Eq. (9) then gives access to the two remaining ones, ΔH_f and B.

The values of ΔH_f thus allow the (n_+/n) ratio to be calculated according to Eq. (2). Now, taking n from density data, the effective charge carrier concentration n_+ is deduced from the (n_+/n) ratio, and the mobility may then be simply calculated from the relation $\mu_+ = \sigma/en_+$, Eq. (1).

Another way to calculate the mobility is given by Eqs. (3) and (4). For this purpose, ν is taken as 10^{13} Hz, the jump distance λ is calculated as the mean distance between two neighboring silver cations $\lambda = \sqrt[3]{1/n}$ (n from density data), and ΔH_m is given by the difference

$$\Delta H_m = E_A - \Delta H_f/2. \tag{10}$$

III. NUMERICAL DETERMINATION OF CHARGE CARRIER CONCENTRATION AND MOBILITY IN THE AgPO₃–AgI SYSTEM

A. Charge carrier formation and migration enthalpies deduced from conductivity data

As mentioned earlier, numerous conductivity measurements have been performed in the xAgI$(1 - x)$AgPO$_3$ system. Among them, we have selected conductivity data of Malugani *et al.*[4] and Pathmanathan *et al.*[7] measured below and above the glass transition temperature, respectively. These authors investigated the same compositions ($x = 0$; 0.1; 0.2; 0.3; 0.4; 0.5), some of which showed overlapping conductivity data below T_g between 200 and 300 K, enabling the coherence of the two sets of measurements to be checked. Original figures of data published by these researchers were digitized and analyzed by DIGITIZEIT software. The collected data have been converted to $\log \sigma T$ and are represented in the same Arrhenius plots in Figure 2.

Experimental data below T_g were extrapolated to determine the pre-exponential term A. The activation energy, E_A,

TABLE I. Parameters A and T_0 and numerical values for ΔH_f and B determined by the best fit of experimental data over the glass transition temperature, using Eq. (9). The values of the pre-exponential term A are determined by extrapolation of σT below T_g using data from Malugani.[4] T_0 are calculated by ($T_0 = 3/4\ T_g$) based on T_g data from Ref. 15. The corresponding number of experimental data points N and χ^2 values are also indicated. The mathematical accuracy is $\pm 10^{-2}$ eV and 3×10^{-3} eV for ΔH_f and B, respectively. x is the AgI molar ratio in the xAgI$(1-x)$AgPO$_3$ glass system.

x	A (KS/cm)	$T_g \pm 5$ (K)	$T_0 \pm 5$ (K)	$\Delta H_f/2$ (eV)	B (eV)	N	χ^2
0	4.2×10^5	459	344	0.43	0.005	126	0.026
0.1	2.13×10^5	436	327	0.34	0.012	162	0.028
0.2	1.4×10^5	419	314	0.30	0.013	84	0.091
0.3	7.7×10^4	393	295	0.24	0.018	134	0.028
0.4	3.8×10^4	375	281	0.17	0.019	82	0.058
0.5	4.6×10^4	353	265	0.13	0.035	91	0.071

FIG. 3. Activation energy (E_A), charge carrier formation (ΔH_f) (as shown in Table I), and migration (ΔH_m) enthalpies as a function of composition in the glass system xAgI$(1-x)$AgPO$_3$. E_A is deduced from conductivity data[4] below T_g. ΔH_m is calculated by the difference as expressed in Eq. (10). The solid lines serve as visual guides.

was obtained using Eq. (6) and data from Malugani *et al.*[4] The data above T_g were fitted by means of Eq. (9) in order to estimate ΔH_f and B. All the calculations were performed using Levenberg-Marquardt nonlinear fitting and ORIGIN™ software. Table I lists, for each composition, the calculated or extrapolated values as well as the number of experimental data points N and respective χ^2 results.

Note that the values of A (Table I) are close to 10^5 K S/cm. This value is in accordance with the estimated one using $A = ne^2\lambda^2 v/6k_B$ (shown in Eq. (6a)), $n = 10^{22}$ ions/cm^3, $\lambda = \sqrt[3]{1/n}$, and $v = 10^{13}$ Hz. The coincidence of the calculated and the extrapolated values indicates that the eventual contribution of the entropies of charge carrier formation and migration is negligible, as postulated previously in Eqs. (2) and (4).

The values of $\Delta H_f/2$ obtained by fitting are formally equivalent to the energy for carrier creation defined by Martin *et al.*[46] It is therefore worth noting that the value of $\Delta H_f/2 = 0.43$ eV found for AgPO$_3$, as indicated in Table I, is consistent with the values of activation energy for carrier creation of 0.50 and 0.45 eV,[46] determined by those authors using space charge polarization measurements in LiPO$_3$ and NaPO$_3$ glasses.

Following the determination of ΔH_f, the migration enthalpy, ΔH_m may be calculated by the difference as shown in Eq. (10). Figure 3 allows for a comparison of the evolution, as a function of AgI content, of the charge carrier formation enthalpy, ΔH_f, their migration enthalpy, ΔH_m, and the activation energy, E_A. E_A is determined using experimental data from Malugani *et al.*[4] A constant decrease of ΔH_f with x is observed, while ΔH_m remains almost constant and close to 0.14 eV in the entire composition range.

B. Charge carrier concentration and mobility

The (n_+/n) ratios at 25 °C calculated using Eq. (2) and ΔH_f values from Table I are presented in Table II.

Once the (n_+/n) ratio has been determined, one needs only the values of the total silver cation concentration n, which may be estimated from density data (Table II), to calculate the concentration of effective charge carrier, n_+. Mobility
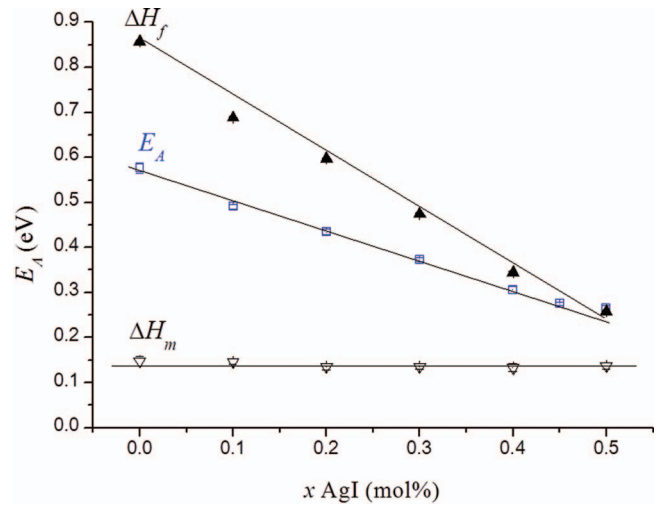
at 25 °C will then be deduced from experimental conductivity data and the relation $\mu_+ = \sigma/en_+$ (Eq. (1)).

As explained in Sec. II of this paper, mobility at room temperature can be calculated by two different procedures. The first one, used above, employs the charge carrier concentration calculated from ΔH_f (Eq. (2)) and experimental conductivity data. The second procedure will use ΔH_m values deduced from the experimental activation energy (Eq. (6b)). Mobility is then calculated using Eqs. (3) and (4). The results at 25 °C obtained by both procedures are similar and listed in Table II. These results do not indicate any tendency of the mobility to depend on the glass composition.

IV. COMPARISON WITH HALL-EFFECT MEASUREMENTS

Using the Hall-effect technique, Clément *et al.*[35] measured mobility at room temperature for the same glass compositions, as investigated here. Mobility obtained by Hall effect and calculated in this work (Table II) is reported in Figure 4. As can be seen, the three data sets are in good agreement. No significant evolution is found as a function of composition. Also, the average of the mobility values measured by the Hall effect, $\langle\mu_{HE}\rangle = 6 \pm 2 \times 10^{-4}$ cm^2 v^{-1} s^{-1}, is very close and intermediate to that calculated in this work, Figure 4: $\langle\mu_+ = 9.4 \times 10^{-4}$ cm^2 V^{-1} s^{-1} (Eqs. (1) and (2)) and $\langle\mu_+ = 4.7 \times 10^{-4}$ cm^2 V^{-1} s^{-1} (Eq. (3)).

The mobility of Ag$^+$ was also measured by the Hall effect in α-AgI (Ref. 33) and in α-RbAg$_4$I$_5$ (Ref. 34). Interestingly, the mobility of silver cation at room temperature was also found to be close to 10^{-4} cm^2 s^{-1} V^{-1} in both investigated materials. It seems, therefore, that charge carrier mobility in an amorphous or crystalline phase is the same, being thus independent of the structure of the host material.

This assumption may justify the result found by the Hall effect[35] and also in this work, i.e., the mobility of Ag$^+$ in the xAgI$(1-x)$AgPO$_3$ is independent of the AgI

TABLE II. Density (from Ref. 24), total silver cation concentration, n, calculated from density data, (n_+/n) ratio, experimental conductivity, σ, and calculated (Eqs. (1) and (2) or Eq. (3)) mobility μ_+ at 25 °C, for the xAgI$(1-x)$AgPO₃ glasses.

AgI molar fraction x	0	0.1	0.2	0.3	0.4	0.5
Density (g/cm³)	4.35	4.56	4.77[a]	4.98	5.20	5.41
Silver cation concentration, n (atom. cm⁻³)	1.12×10^{22}	1.19×10^{22}	1.28×10^{22}	1.36×10^{22}	1.45×10^{22}	1.54×10^{22}
(n_+/n) (25 °C)	6.25×10^{-8}	1.65×10^{-6}	9.59×10^{-6}	1.04×10^{-4}	1.29×10^{-3}	6.79×10^{-3}
σ (25 °C) (S cm⁻¹) (experimental)	2.40×10^{-7}	1.91×10^{-6}	2.19×10^{-5}	1.26×10^{-4}	8.71×10^{-4}	5.13×10^{-3}
μ_+ (25 °C) (cm²/V s) (Eqs. (1) and (2))	25×10^{-4}	5.7×10^{-4}	13×10^{-4}	6.6×10^{-4}	2.8×10^{-4}	3.3×10^{-4}
μ_+ (25 °C), (cm²/V s) (Eq. (3))	3.8×10^{-4}	3.6×10^{-4}	5.1×10^{-4}	4.9×10^{-4}	6.9×10^{-4}	4.5×10^{-4}

[a]Interpolated value.

content, x. As a consequence, the variation in ionic conductivity with composition is attributable mainly to the variation in the number of effective charge carriers.

V. THERMODYNAMICS OF CHARGE CARRIERS

According to the results presented in Table II, Sec. IV, the large isothermal increase in conductivity with silver iodide content cannot be related to an increase in charge carrier mobility, which is not dependent on the composition. It is therefore more likely the result of a significant increase in the number of effective charge carriers. These variations can be validated from dissociation equilibria analogous to those developed for the study of weak electrolyte solutions.[38,39]

In the present case, we will consider the xAgI$(1-x)$AgPO₃ glass system as a solution of AgI dissolved in AgPO₃. Since the dissolution of silver iodide increases the ionic conductivity of pure silver phosphate by several orders of magnitude, we can assume that the partial dissociation of AgI predominates, at $0.1 \leq x \leq 0.5$, over that of AgPO₃. Accordingly, AgI dissociation produces a much higher number of effective silver charge carriers than those originating from the vitreous solvent AgPO₃. Thus, we will consider only the dissociation equilibrium of AgI, which can be written as follows:
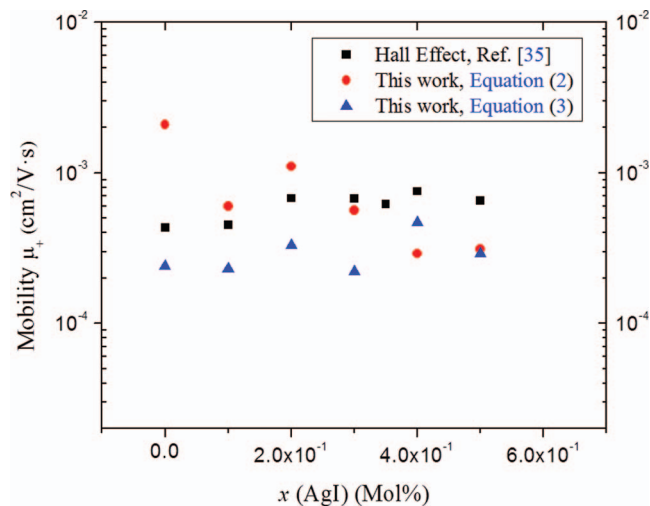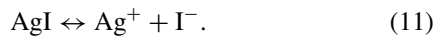
$$AgI \leftrightarrow Ag^+ + I^-. \tag{11}$$

FIG. 4. Room temperature mobility μ_+ calculated in this work from conductivity data and Eqs. (2) [●] and (3) [▲] and measured by the ionic Hall effect[35] [■], for xAgI$(1-x)$AgPO₃ glasses.

In the glassy state, the species Ag⁺ is identified as a silver cation in an interstitial position and the I⁻ anion is considered as a vacant silver site. This dissociation equilibrium is associated to a dissociation constant, $K = \exp(-\Delta G_f^0 / k_B T)$, in which ΔG_f^0 is the standard free energy of charge carrier (Ag⁺) formation in the vitreous solvent. The reference states are arbitrary. In the present case, the Ag⁺ and I⁻ ions are taken at infinite dilution, allowing the ion activity to be assimilated to their concentrations; hence,

$$k_B T \ln[Ag^+][I^-] = -\Delta G_f^0 + \overline{\Delta G}_{AgI},$$

where $\overline{\Delta G}_{AgI}$ is the difference in the partial free energy of AgI in the reference state and in the glass composition under study.

Since $[Ag^+] = [I^-] = (n_+/n)$, it follows that the number of effective charge carriers, n_+, is an exponential function of the partial free energy, $\overline{\Delta G}_{AgI}$, and can be written as

$$n_+ = n \exp\left(\frac{-\Delta G_f^0 + \overline{\Delta G}_{AgI}}{2k_B T}\right). \tag{12}$$

The factor 2 in the exponent indicates that the dissociation process generates two charged species, a charge carrier (Ag⁺) and its vacant site (I⁻), both in the same concentration.

Finally, since the mobility term can be considered a constant, the variation in ionic conductivity according to x should follow the variations in the partial free energy of silver iodide with x, according to

$$\log \sigma \propto \log n_+ \propto \frac{\overline{\Delta G}_{AgI}}{2.3 \times 2k_B T} + cte = \frac{1}{2}\log a_{AgI} + cte, \tag{13}$$

where a_{AgI} is defined as the thermodynamic activity of silver iodide.

In a previous work,[11] the thermodynamic activity of silver iodide in the xAgI$(1-x)$AgPO₃ glass system was estimated from dissolution calorimetry data. In this case, the relationship between the conductivity and thermodynamic activity of AgI (Eq. (13)) between $x = 0.2$ and $x = 0.45$ was well verified.

In this work, in order to find a relationship between $\overline{\Delta G}_{AgI}$ and the glass composition, we make the simple assumption of a regular solution of AgI and AgPO₃. This model is generally found valid for molten salt solutions of two salts of the same cation and different anions[47,48] and has been used to explain observed conductivity enhancement by dissolution
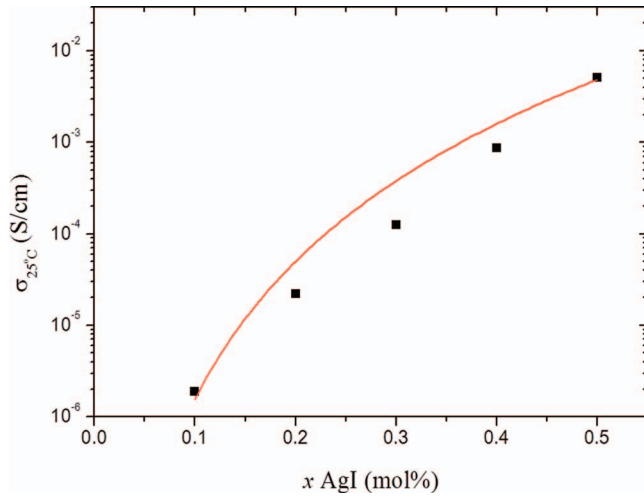
FIG. 5. Ionic conductivity of the glass system xAgI$(1 - x)$AgPO$_3$ at 25 °C. Symbols represent experimental data from Malugani *et al.*[4] The solid line represents the expected variation from a regular solution model (see text) with $\alpha = 81.5$ kJ mol^{-1}.

FIG. 6. Activation energy for conduction in the glass system xAgI$(1 - x)$AgPO$_3$. The symbols represent experimental data from Malugani *et al.*[4] The solid line corresponds to the expected variation from a regular solution model (see text) with $\alpha = 82$ kJ mol^{-1}.

of halide salts in inorganic glasses.[39] The mixture of the two components entails a mixing free energy, which is expressed as a function of x by

$$\Delta G_{mix} = -\alpha\, x(1 - x) + k_B T[x \ln x + (1 - x)\ln(1 - x)]. \tag{14}$$

In this expression, the first term corresponds to the mixing enthalpy, $\Delta H_{mix} = -\alpha\, x(1 - x)$ in which α is an interaction parameter representative of the ionic bond rearrangement resulting from the dissolution of AgI in AgPO$_3$. The second term is the ideal configurational mixing entropy, $-T\Delta S_{mix}$. Using the Gibbs-Duhem relation, this expression leads to the following expression for the partial free energy of silver iodide with x:

$$\overline{\Delta G}_{\text{AgI}} = \Delta G_{mix} + (1 + x)\frac{\partial \Delta G_{mix}}{\partial x} = k_B T \ln x - \alpha(1 - x)^2. \tag{15}$$

According to Eqs. (13) and (15), isothermal variations in conductivity follow the relation

$$\log \sigma \propto \frac{\overline{\Delta G}_{\text{AgI}}}{2.3 \cdot 2k_B T} = \frac{1}{2}\log x - \frac{\alpha(1 - x)^2}{2.3 \times 2k_B T}. \tag{16}$$

Thus, by fitting experimental isothermal conductivity variations with Eq. (16), it is possible to determine the corresponding value for the interaction parameter α. Such a fit is shown in Figure 5 for $0.1 \leq x \leq 0.5$ and determines a value of 81.5 kJ mol^{-1} for the α parameter.

The α parameter can also be calculated from the variation, with x, of the activation energy E_A. According to Eqs. (6b) and (12),

$$E_A = \Delta H_f/2 + \Delta H_m = \left(\frac{\Delta H_f^0 - \overline{\Delta H}_{\text{AgI}}}{2}\right) + \Delta H_m. \tag{17}$$
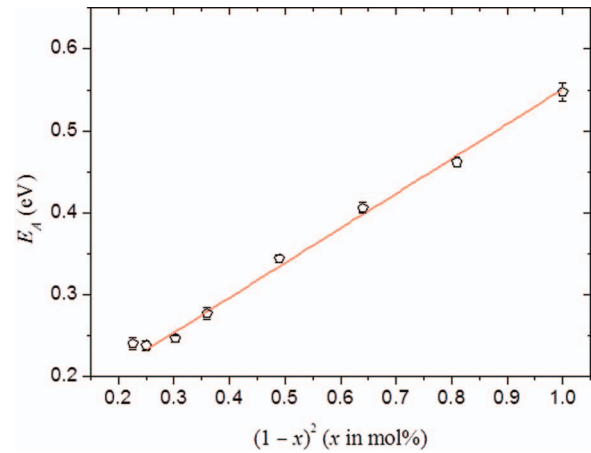
Since our results indicate that the migration enthalpy ΔH_m does not depend on x (Figure 3), then

$$E_A = cte - \frac{\overline{\Delta H}_{\text{AgI}}}{2} \propto \frac{\alpha(1 - x)^2}{2}. \tag{18}$$

Variations of E_A as a function of $(1 - x)^2$ are illustrated in Figure 6 and define a straight line whose slope indicates a value of $\alpha = 82$ kJ mol^{-1}, which is identical to the value determined from the fit of isothermal conductivity variations using Eq. (16).

The positive value found for the α parameters corresponds, for $x = 0.5$, to a negative molar enthalpy of mixing of -20 kJ mol^{-1}. This value is representative of strong interactions between the AgPO$_3$ chains and the dissolved AgI, which compensate for the reticular energy of crystalline AgI, thus allowing for the dissolution of silver iodide in silver phosphate.

Previous Raman,[22] neutron diffraction,[26] and ^{31}P NMR studies[16] indicate that this dissolution does not modify the structure of phosphate chains in the host glass. The first structural hypothesis about the dissolved AgI suggested that it would form clusters of a structure similar to that of the fast ion conductor α-AgI. When interconnected, these clusters would form preferential pathways for silver cations,[25,28,29] thereby enhancing the conductivity. This model was later disavowed by more recent structural studies using EXAFS, neutron, and x-ray diffraction coupled with a reverse Monte Carlo method.[31] The latter studies confirmed that the silver iodide is completely dispersed in the phosphate matrix and that silver cations undergo mixed oxygen-iodine coordination.[20,23]

We may thus reasonably suggest that silver iodide interacts with ionic silver phosphate bonds through strong electrostatic dipole-dipole interactions, which explain the relatively high value for the α parameter. This ionic interaction between silver iodide and phosphate chains would simultaneously diminish the electrostatic interactions among the phosphate chains themselves and explain the significant drop in

the glass transition temperature resulting from the addition of a halide salt.[4,13,15]

A good agreement can be also noted in Figures 5 and 6 between experimental data and the corresponding conductivity variations deduced from the regular solution model. This agreement validates both the weak electrolyte and the thermodynamic model employed here to describe the AgI–AgPO₃ glassy solutions and the dependence of their electrical conductivity and activation energy on composition.

VI. CONCLUSION

Experimental electrical conductivity data of the xAgI $(1 - x)$AgPO₃ glass system were collected from the literature. The drastic change in conductivity at the glass transition temperature, T_g, is interpreted based on a change in the mobility mechanism. According to this hypothesis, the analysis of the conductivity data with temperature below and above T_g allows the enthalpies involved in charge carrier formation and migration to be determined in the glassy state. Thus, the enthalpy of charge carrier formation enables us to calculate the charge carrier concentration, and hence, mobility as a function of temperature and composition ($0 \leq x \leq 0.5$). At a constant temperature, charge carrier mobility appears to be independent of the glass composition, i.e., the AgI content. These results, found close to 10^{-4} cm² V⁻¹ s⁻¹ at room temperature, are in good agreement with the mobility measured directly by the Hall-effect technique.

The strong dependence of ionic conductivity on the AgI content, which shows an increase at room temperature of about four orders of magnitude when x varies from 0 to 0.5, can therefore only be attributed to an increase of the same order of magnitude in the charge carrier concentration.

Our interpretation considers the xAgI$(1-x)$AgPO₃ glasses as weak electrolytes, with the charge carriers resulting from the partial dissociation of silver iodide in the AgPO₃ solvent. Variations in conductivity as a function of composition are thus correlated to the partial free energy of AgI in the AgI–AgPO₃ mixture, which is described as a regular solution with an interaction parameter of 82 kJ mole⁻¹.

[1] E. Kartini, T. Y. S. P. Putra, I. Kuntoro, T. Sakuma, K. Basar, O. Kamishima, and J. Kawamura, J. Phys. Soc. Jpn. **79** (Suppl. A), 54 (2010).

[2] J.-P. Malugani, B. Fahys, R. Mercier, G. Robert, J. P. Duchange, S. Banstry, M. Broussely, and J. P. Gabano, Solid State Ionics **9–10**, 659 (1983).

[3] J.-P. Malugani, A. Wasniewski, M. Doreau, and G. Robert, C. R. Acad. Sc. Paris, Ser. C **283**, 111 (1976).

[4] J.-P. Malugani, A. Wasniewski, M. Doreau, G. Robert, and A. Al Rikabi, Mater. Res. Bull. **13**, 427 (1978).

[5] M. B. M. Mangion and G. P. Johari, Phys. Chem. Glasses **29**, 225 (1988).

[6] C. Liu and C. A. Angell, J. Non-Cryst. Solids **83**, 162 (1986).

[7] K. Pathmanathan, R. Mlcak, and G. P. Johari, Phys. Chem. Glasses **30**, 180 (1989).

[8] M. Le Stanguennec and S. R. Elliot, Solid State Ionics **73**, 199 (1994).

[9] B. Roling, M. D. Ingram, M. Lange, and K. Funke, Phys. Rev. B **56**(21), 13619 (1997).

[10] M. Cutroni, A. Mandanici, P. Mustarelli, and C. Tomasi, Solid State Ionics **154–155**, 713 (2002).

[11] J.-C. Reggiani, J.-P. Malugani, and J. Bernard, J. Chim. Phys. **75**(3), 245 (1978).

[12] A. Shiraldi, E. Pezzati, P. Baldini, and S. W. Martin, Solid State Ionics **18–19**, 426 (1986).

[13] A. Hallbrucker and G. P. Johari, Phys. Chem. Glasses **30**, 211 (1989).

[14] M. Nakayama, M. Hanaya, A. Hatate, and M. Oguni, J. Non-Cryst. Solids **172–174**, 1252 (1994).

[15] S. K. Lee, M. Tatsumisago, and T. Minami, J. Ceram. Soc. Jpn. **102**, 84 (1994).

[16] S. Hayashi and K. Hayamizu, J. Solid State Chem. **80**, 195 (1989).

[17] K. K. Olsen, J. Zwanziger, P. Hartmann, and C. Jäger, J. Non-Cryst. Solids **222**, 199 (1997).

[18] C. Tomasi, P. Mustarelli, A. Magistris, and Ma. P. I. Garcia, J. Non-Cryst. Solids **293–295**, 785 (2001).

[19] P. Mustarelli, C. Tomasi, A. Magistris, and L. Linati, Phys. Rev. B **63**, 144203 (2001).

[20] J. Kawamura, N. Kuwata, Y. Nakamura, T. Erata, and T. Hattori, Solid State Ionics **154–155**, 183 (2002).

[21] J.-P Malugani and R. Mercier, Solid State Ionics **13**, 293 (1984).

[22] M. Villa, G. Chiodelli, and M. Scagliotti, Solid State Ionics **18–19**, 382 (1986).

[23] E. I. Kamitsos, J. A. Kapoutsis, G. D. Chryssikos, J. M. Hutchinson, A. J. Pappin, M. D. Ingram, and J. A. Duffy, Phys. Chem. Glasses **36**, 141 (1995).

[24] L. Borjesson, S. W. Martin, L. M. Torell, and C. A. Angell, Solid State Ionics **18–19**, 431 (1986).

[25] M. Tachez, R. Mercier, J. P. Malugani, and A. J. Dianoux, Solid State Ionics **20**, 93 (1986).

[26] M. Tachez, R. Mercier, J.-P. Malugani, and P. Chieux, Solid State Ionics **25**, 263 (1987).

[27] R. Mercier, M. Tachez, J. P. Malugani, and C. Rousselot, Mater. Chem. Phys. **23**, 13 (1989).

[28] L. Börjesson and W. S. Howells, Solid State Ionics **40–41**, 702 (1990).

[29] C. Rousselot, M. Tachez, G. P. Malugani, R. Mercier, and P. Chieux, Solid State Ionics **44**, 151 (1991).

[30] C. Rousselot, G. P. Malugani, R. Mercier, M. Tachez, P. Chieux, A. J. Pappin, and M. D. Ingram, Solid State Ionics **78**, 211 (1995).

[31] J. Swenson, R. l. McGreevy, L. Börjesson, and J. D. Wicks, Solid State Ionics **105**, 55 (1998).

[32] A. Matic, J. Swenson, L. Börjesson, S. Longeville, R. E. Lechner, W. S. Howells, T. Akai, and S. W. Martin, Physica B **266**, 69 (1999).

[33] K. Funke and R. Hackenberg, Ber. Bunsenges. Phys. Chem. **76**, 883 (1972).

[34] C. H. J. Stuhrmann, H. Kreiterling, and K. Funke, Solid State Ionics **154–155**, 109 (2002).

[35] V. Clément, D. Ravaine, C. Déportes, and R. Billat, Solid State Ionics **28–30**, 1572 (1988).

[36] J. L. Souquet, A. C. M. Rodrigues, and M. L. F. Nascimento, J. Chem. Phys. **132**, 034704 (2010).

[37] E. Caillot, M. J. Duclot, J. L. Souquet, M. Levy, E. G. K. Baucke, and R. Werner, Phys. Chem. Glasses **35**, 22 (1994).

[38] D. Ravaine and J. L. Souquet, Phys. Chem. Glasses **18**, 27 (1977).

[39] A. Kone and J.-L. Souquet, Solid State Ionics **18–19**, 454 (1986).

[40] R. G. Charles, J. Appl. Phys. **32**, 1115 (1961).

[41] Y. Haven and B. Verkerk, Phys. Chem. Glasses **6**, 38 (1965).

[42] M. D. Ingram, M. A. Mackenzie, and A. V. Lesikar, J. Non-Cryst. Solids **38–39**, 371 (1980).

[43] M. H. Cohen and D. Turnbull, J. Chem. Phys. **31**, 1164 (1959).

[44] G. Adam and J. H. Gibbs, J. Chem. Phys. **43**, 139 (1965).

[45] J. W. P. Schmelzer and I. Gutzow, *Glasses and the Glass Transition* (Wiley VCH, Berlin, 2011).

[46] S. W. Martin, W. Yao, and K. Berg, Z. Phys. Chem. **223**, 1379 (2009).

[47] J. Lumdsen, *Thermodynamics of Molten Salt Mixtures* (Academic, New York, 1966).

[48] G. Mamantov, *Molten Salt Chemistry*, Nato Science Series C Vol. 202 (Springer, New York, 1987).